

Robert S. Rogers,¹ E. Matthew Morris,¹ Joshua L. Wheatley,¹ Ashley E. Archer,¹ Colin S. McCain,¹ Kathleen S. White,¹ David R. Wilson,¹ Grace M.E. Meers,² Lauren G. Koch,³ Steven L. Britton,^{3,4} John P. Thyfault,^{1,5} and Paige C. Geiger¹



Deficiency in the Heat Stress Response Could Underlie Susceptibility to Metabolic Disease

Diabetes 2016;65:3341–3351 | DOI: 10.2337/db16-0292

Heat treatment (HT) effectively prevents insulin resistance and glucose intolerance in rats fed a high-fat diet (HFD). The positive metabolic actions of heat shock protein 72 (HSP72), which include increased oxidative capacity and enhanced mitochondrial function, underlie the protective effects of HT. The purpose of this study was to test the ability of HSP72 induction to mitigate the effects of consumption of a short-term 3-day HFD in rats selectively bred to be low-capacity runners (LCRs) and high-capacity runners (HCRs)—selective breeding that results in disparate differences in intrinsic aerobic capacity. HCR and LCR rats were fed a chow or HFD for 3 days and received a single in vivo HT (41°C, for 20 min) or sham treatment (ST). Blood, skeletal muscles, liver, and adipose tissues were harvested 24 h after HT/ST. HT decreased blood glucose levels, adipocyte size, and triglyceride accumulation in liver and muscle and restored insulin sensitivity in glycolytic muscles from LCR rats. As expected, HCR rats were protected from the HFD. Importantly, HSP72 induction was decreased in LCR rats after only 3 days of eating the HFD. Deficiency in the highly conserved stress response mediated by HSPs could underlie susceptibility to metabolic disease with low aerobic capacity.

Low aerobic capacity is a strong independent predictor of metabolic syndrome, type 2 diabetes, cardiovascular disease, and all-cause mortality, even when traditional risk factors, such as smoking and obesity, are considered (1–5). The mechanisms underlying the relationship between low

intrinsic aerobic capacity and susceptibility to chronic metabolic disease remain largely unknown. Interestingly, an estimated 50–70% of an individual's aerobic capacity, and thus disease risk, can be attributed to inheritable traits (6). Heat shock proteins (HSPs) strongly correlate with oxidative capacity in skeletal muscle and adipose tissue (7–9), and may also underlie innate differences in susceptibility to metabolic disease.

The heat shock response is a highly conserved defense system to combat cellular and oxidative stress (10,11), and involves the induction of a family of HSPs identified by molecular weight (11). Kurucz et al. (12) first demonstrated that HSP72 expression was markedly decreased in the skeletal muscle of patients who are insulin resistant and have type 2 diabetes. Subsequent studies (13–17) showed that heat treatment (HT), transgenic overexpression of HSP72, and pharmacological induction of HSP72 effectively prevent high-fat diet (HFD)–induced glucose intolerance and skeletal muscle insulin resistance. Interestingly, the overexpression of skeletal muscle HSP72 in mice has been shown to increase endurance running capacity nearly twofold and to increase mitochondrial content by 50% (15). We hypothesize that the ability of HSPs to improve glucose homeostasis and increase oxidative capacity may provide protection against short-term metabolic insult. Furthermore, we hypothesize that elevated HSP responses may play a role in the protective phenotype associated with elevated aerobic capacity.

Rats bred to be low-capacity runners (LCRs) display symptoms of metabolic disease, including glucose intolerance,

¹Department of Molecular and Integrative Physiology, University of Kansas Medical Center, Kansas City, KS

²Department of Medicine–Gastroenterology and Hepatology, University of Missouri, Columbia, MO

³Department of Anesthesiology, University of Michigan, Ann Arbor, MI

⁴Department of Molecular and Integrative Physiology, University of Michigan, Ann Arbor, MI

⁵Research Service, Kansas City VA Medical Center, Kansas City, MO

Corresponding author: Paige C. Geiger, pgeiger@kumc.edu.

Received 1 March 2016 and accepted 16 August 2016.

This article contains Supplementary Data online at <http://diabetes.diabetesjournals.org/lookup/suppl/doi:10.2337/db16-0292/-/DC1>.

© 2016 by the American Diabetes Association. Readers may use this article as long as the work is properly cited, the use is educational and not for profit, and the work is not altered. More information is available at <http://www.diabetesjournals.org/content/license>.

skeletal muscle insulin resistance, and increased hepatic triglyceride storage (18–23). In contrast, rats bred to be high-capacity runners (HCRs) are protected against HFD-induced metabolic conditions. To date, the role of HSPs in modulating susceptibility of HCRs and LCRs to metabolic disease has not been examined (18,20–24). As a result, the purpose of this study was to test our hypothesis regarding the ability of HSP induction via HT to protect against a short-term metabolic insult in LCR rats. Our results demonstrate the beneficial metabolic effects of HT in multiple tissues; however, a diminished HSP response in LCR rats could increase susceptibility to long-term HFD feeding and metabolic disease.

RESEARCH DESIGN AND METHODS

Animal Strains

The development of LCR and HCR rats has been described previously (18,25). Animal protocols were approved by the Institutional Animal Care and Use Committees at the University of Kansas Medical Center, the University of Michigan, and the University of Missouri, as well as by the Subcommittee for Animal Safety at the Harry S. Truman Memorial VA Hospital.

Seven-month-old male LCR and HCR rats ($n = 48$; generation 25) were housed in a temperature-controlled facility with 12-h light/dark cycles, and were provided with standard rat chow and water available ad libitum upon arrival. Rats were acclimated to the low-fat control diet (D12450B, 10% kcal from fat; Research Diets, New Brunswick, NJ) for ≥ 7 days prior to initiation of the experimental diet period. Rats continued to be fed either the low-fat control diet or were placed on an HFD (D12451 [45% of kilocalories from fat]; Research Diets) for 3 days. After 3 days, rats were anesthetized with short-acting ketamine-xylazine (80 mg/kg body wt/10 mg/kg body wt) and received a single in vivo HT or sham treatment (ST), as previously described (9,14). Twenty-four hours after HT or ST, and after a 10-h overnight fast, rats were anesthetized with pentobarbital sodium (5 mg/100 g body wt), an anesthetic that does not result in hyperglycemia (26), and tissues were dissected. Data in Supplementary Fig. 1 were taken from animals in generation 30. This subset of animals were fed the same 3-day chow diet and HFD, but HT/ST was not performed. Body weight, feeding, energy consumption, and liver parameters for animals in generation 30 have been reported elsewhere (22).

Blood Measures

Fasting blood glucose concentration was measured using a glucose analyzer and manufacturer test strips (Accu-Chek Active; Roche Diagnostics, Indianapolis, IN).

Adipose Tissue Imaging

Epididymal white adipose tissue (eWAT) was fixed overnight in 4% paraformaldehyde, placed in 70% ethanol for 48–72 h, processed, and paraffin embedded for hematoxylin-eosin staining. Images were taken on a Nikon 80i microscope and quantified using ImageJ.

Glucose Transport

Insulin-stimulated glucose transport into soleus and extensor digitorum longus (EDL) muscle strips was determined as previously described (14).

Intramuscular Triglyceride Content

Muscle and liver tissue triglyceride content was determined by methods described previously (27,28).

Primary Muscle Cultures and Glucose Transport

Primary myoblasts were isolated from adult male HCR and LCR rats ($n = 8$; generation 37), and male Wistar rats, as previously described (29). Briefly, quadriceps, gastrocnemius, EDL, and tibialis anterior muscles were dissected, and finely minced for digestion in protease buffer with 1% collagenase and growth media (Ham's F-10, 20% FBS, 1% penicillin/streptomycin/gentamycin). Cells were placed in T150 flasks to optimize growth and then on six-well plates in DMEM containing 4.5 g/L glucose, 10% horse serum (HS), and 1% penicillin/streptomycin/gentamycin. After 4–5 days, myoblasts were differentiated into skeletal muscle cells in DMEM containing 1 g/L glucose, 2% HS, and 1% penicillin/streptomycin. Twenty-four and 48 h after differentiation, myotubes were transfected using MISSION small interfering RNA (siRNA) transfection reagent with either HSP72-specific siRNA (catalog #NM-212504; Sigma-Aldrich, St. Louis, MO) or scrambled sequence as a negative control. Twenty-four hours after the second transfection, all myotubes were subjected to HT by placing plates in a 42°C water bath for 30 min and then returning them to conditions of 37°C with 5% CO₂. Glucose transport experiments were performed 24 h after HT. Myotubes were serum starved for 6 h prior to experiments and then exposed to insulin (12 nM) or no insulin for 1 h. Media was aspirated, and myotubes were incubated with (³H)2-deoxyglucose (1 μ Ci) for 10 min. Cells were washed with ice-cold PBS to stop the reaction, myotubes were lysed in 0.5 mL of 0.03% SDS buffer, and radioactivity was counted on a scintillation counter. Each experiment was performed with $n = 6$ per treatment group and repeated three times.

Western Blotting

Muscles, liver, adipose tissue, and myotubes were processed for Western blotting by methods previously described (9,30). Primary antibodies used included HSP72 (catalog #SPA-810; Enzo Life Sciences, Farmingdale, NY), HSP60 (catalog #SPA-807; Stressgen), heat shock factor-1 (HSF-1; catalog #NB300-730; Novus Biochemicals, Littleton CO), PGC-1 α (peroxisome proliferator-activated receptor γ coactivator-1 α ; catalog #516557; Calbiochem, Darmstadt, Germany), HSP25 (catalog #SPA-801; Stressgen), α -tubulin (catalog #ab7291; Abcam, Cambridge, MA), β -actin horseradish peroxidase-conjugated (catalog #ab20272; Abcam), MitoProfile Total OXPHOS (catalog #ab110413; Abcam), Sirt1 (catalog #ab20272; Abcam), mtFAM (catalog #sc-23588; Santa Cruz Biotechnology, Dallas, TX), Parkin (catalog #sc-32282; Santa Cruz Biotechnology), phospho-AS160

(Thr642) (catalog #4288; Cell Signaling Technology, Danvers, MA), phospho-Akt (Ser473) (catalog #9271; Cell Signaling Technology), total Akt (catalog #9272; Cell Signaling Technology), and total AS160 (catalog #ABS54; Millipore, Billerica, MA). Secondary antibodies used included goat anti-rabbit (catalog #sc-2004; Santa Cruz Biotechnology), goat anti-mouse (catalog #170-5047; Bio-Rad, Hercules, CA), rabbit antirat (catalog #A-5795; Sigma-Aldrich), rabbit anti-goat (catalog #A-5420; Sigma-Aldrich), and donkey anti-rabbit (Jackson ImmunoResearch, West Grove, PA).

Statistical Analyses

Results are presented as the mean \pm SEM. Statistical significance was set at $P < 0.05$. Analysis was performed using SigmaPlot for Windows, version 12.0 (Systat Software Inc., Chicago, IL). Data were analyzed by one-way or two-way ANOVAs with Fisher LSD post hoc comparisons performed where appropriate, as noted.

RESULTS

Body Composition, Energy Intake, and Blood Glucose

As previously reported (22), initial body weight was greater in LCR rats compared with HCR rats, and although both strains increased body weight during the HFD, the LCR rats gained significantly more during the 3-day HFD (Table 1). Food and energy intake were greater in LCR rats compared with HCR rats. However, when normalized to body weight, energy intake was not significantly different between LCR/HCR rats after a 3-day HFD. Food intake and energy intake of HFD-fed LCR rats were greater than HFD-fed HCR rats. Compared phenotypically, fasting blood glucose levels were greater in LCR rats compared with HCR rats (135.9 ± 2.6 vs. 112.6 ± 3.4 mg/dL, for LCR vs. HCR, respectively; $P < 0.05$), and there was no effect of diet on blood glucose level in either strain. Importantly, HT reduced blood glucose concentrations in chow-fed LCR

rats (138.9 ± 2.9 to 125.8 ± 2.3 mg/dL, $P < 0.05$) and in HFD-fed LCR rats (132.9 ± 2.4 to 124.6 ± 4.6 mg/dL, $P < 0.05$), whereas no effect of HT was observed on HCR blood glucose levels.

Insulin Action Is Improved With HT in LCR Glycolytic Muscles

In the EDL muscle, insulin-stimulated glucose uptake was not significantly different between HCR and LCR rats being fed the chow diet; however, basal glucose uptake (Fig. 1A, open bars) was greater in HCR rats compared with LCR rats. The 3-day HFD reduced insulin-stimulated glucose uptake in the EDL muscle from LCR rats, and this was restored by short-term HT. Similarly, insulin-stimulated phosphorylation of Akt substrate of 160 kDa (AS160) was decreased in EDL muscles from LCR rats after a 3-day HFD and was restored by HT (Fig. 1B). Insulin-stimulated Akt phosphorylation in the EDL was not different between HCR/LCR rats and was not altered after HFD or HT (Fig. 1C). Unlike in the EDL muscle, insulin-stimulated glucose uptake in the soleus was greater in HCR rats compared with LCR rats (Fig. 1E), while soleus muscle glucose uptake was not impacted by the 3-day HFD or changed after HT in either rat strain. Similar to the glucose uptake pattern, insulin-stimulated Akt ($P < 0.05$) and AS160 ($P < 0.06$) phosphorylation were higher in soleus muscles from HCR compared with LCR (Fig. 1F and 1G). Due to a limited sample size after processing muscles for glucose uptake, only HCR vs. LCR insulin signaling was assessed. However, we would not expect to see diet and HT effects on phospho-Akt and phospho-AS160 given the lack of changes in glucose uptake in this muscle.

HSP Induction in Glycolytic and Oxidative Muscles From HCR/LCR Rats

HT results in induction of HSP72 protein expression in EDL and soleus muscles from HCR rats and this was not

Table 1—Body weight, organ weights, and feeding characteristics for HCR and LCR rats from generation 25 after 3 days of being fed an HFD

	HCR		LCR	
	Control diet	HFD	Control diet	HFD
Body weight (g)	364.3 \pm 11.2	358.3 \pm 10.0	464.9 \pm 14.5*	455.6 \pm 12.7*
3-Day daily weight gain (g/day)	0.5 \pm 0.4	1.5 \pm 0.4†	1.4 \pm 0.2*	5.8 \pm 0.5*†#
Food intake (g/day)	15.9 \pm 0.6	17.8 \pm 0.8†	19.3 \pm 0.8*	22.5 \pm 0.8*†
Energy intake (kcal/day)	61.4 \pm 2.4	84.0 \pm 3.5†	74.2 \pm 3.2*	106.3 \pm 3.7*†
Energy intake (kcal/day)/body weight (g)	0.17 \pm 0.01	0.24 \pm 0.01†	0.16 \pm 0.01	0.23 \pm 0.01†
Soleus muscle (mg)/body weight (g)	0.65 \pm 0.02	0.72 \pm 0.02†	0.52 \pm 0.03*	0.56 \pm 0.02*†
EDL muscle (mg)/body weight (g)	0.52 \pm 0.01	0.51 \pm 0.01	0.43 \pm 0.01*	0.43 \pm 0.01*
Gastrocnemius muscle (mg)/body weight (g)	5.94 \pm 0.14	5.98 \pm 0.09	5.08 \pm 0.14*	5.09 \pm 0.14*
Tibialis anterior muscle (mg)/body weight (g)	1.97 \pm 0.03	2.02 \pm 0.04	1.65 \pm 0.05*	1.66 \pm 0.03*
Heart muscle (mg)/body weight (g)	2.85 \pm 0.07	2.90 \pm 0.07	2.63 \pm 0.06*	2.60 \pm 0.08*

Data are reported as the mean \pm SEM. Body weight prior to 3-day HFD consumption, body weight gain, percentage of muscle weights relative to body mass, and feeding characteristics of HCR/LCR rats from generation 25. * $P < 0.001$ denotes a significant main effect of strain; † $P < 0.05$ –0.001 denotes a significant main effect of diet; # $P < 0.001$ denotes a significant strain \times diet interaction assessed by two-way ANOVA, with Fisher LSD post hoc comparisons where appropriate.

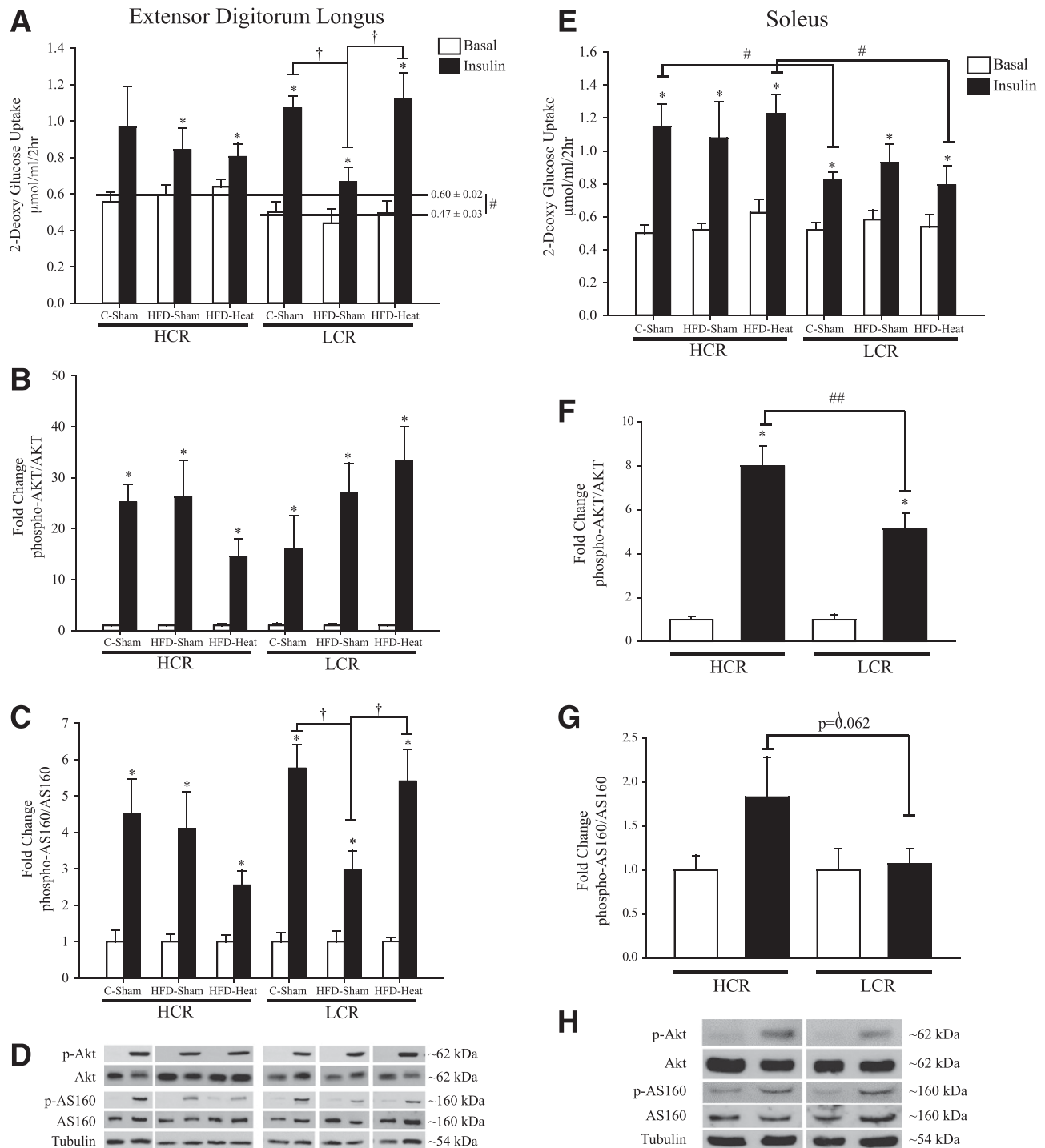


Figure 1—Skeletal muscle insulin responsiveness in EDL and soleus muscles of HCR/LR rats. Insulin-stimulated glucose uptake in EDL muscle (A) and soleus muscle (E) and phosphorylation of Akt (B and F) and AS160 (C and G) in HCR/LCR rats fed either a chow diet (C) or a 3-day HFD and receiving a single *in vivo* ST (37°C) or HT (41°C). D and H: Representative blots of phosphorylated (p)-Akt/Akt and p-AS160/AS160 in EDL and soleus muscles. White bars represent the basal condition, and black bars represent the insulin-stimulated condition. * $P < 0.05$ –0.001 denotes significantly different from basal condition; # $P < 0.05$, ## $P < 0.01$ denotes that HCR/LCR rats are significantly different; † $P < 0.05$ denotes that LCR HFD-ST rats had significantly lower insulin-stimulated glucose uptake than LCR C-ST rats and LCR HFD-HT rats determined by one-way ANOVA. Values are reported as the mean \pm SE. $N = 3$ –6 animals/group.

altered by a 3-day HFD (Fig. 2A and B). HT resulted in an increase in HSP72 protein expression in the EDL muscles from LCR rats, however this induction was blunted with a 3-day HFD (33% decrease). Interestingly, induction of

HSP72 was not observed in soleus muscles from LCR rats even on a chow diet. Constitutive HSP72 levels were greater in the EDL of HCR rats compared with LCR rats, while constitutive HSP72 expression in the soleus muscle was

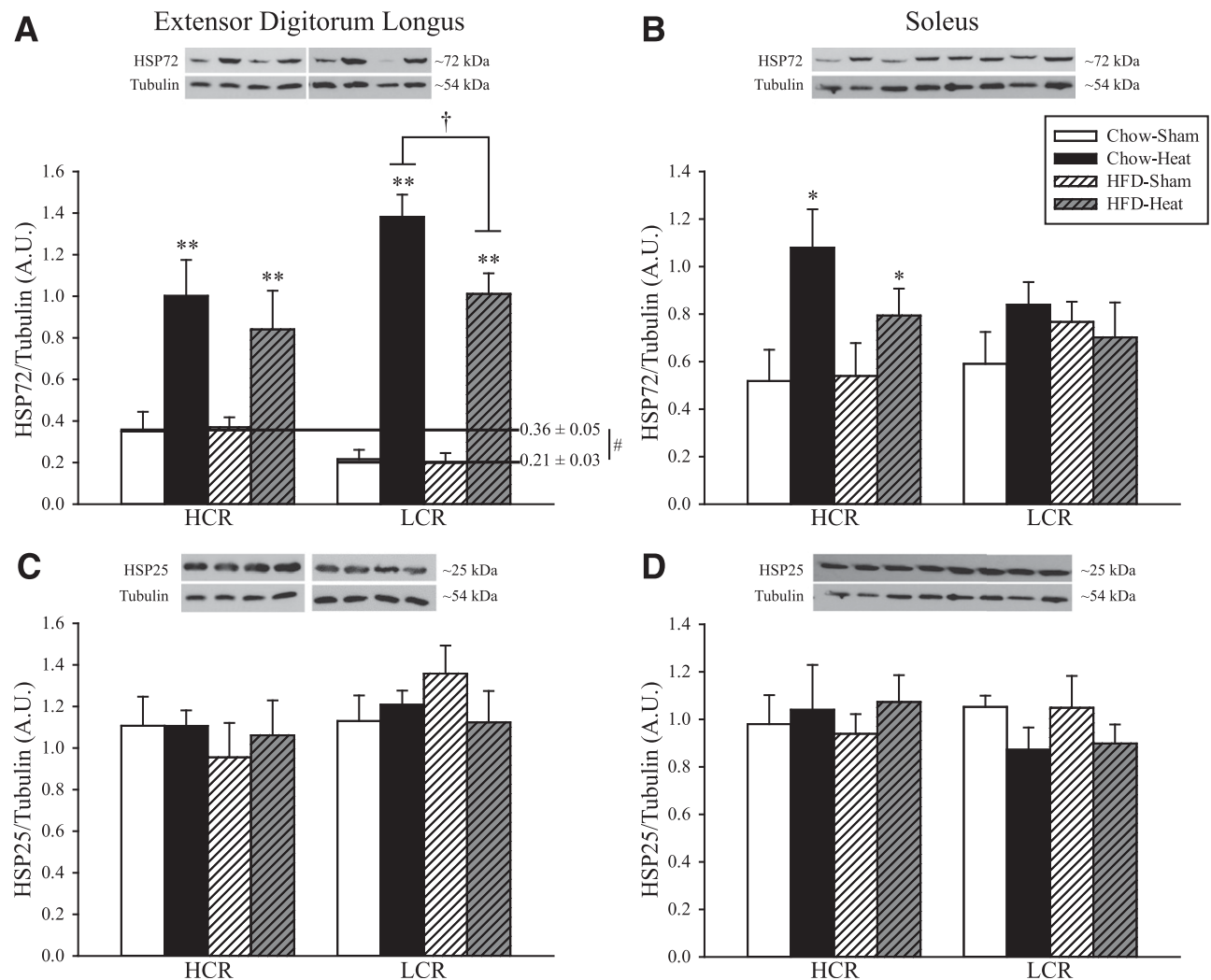


Figure 2—Heat shock response in skeletal muscle of HCR/LCR rats. HSP72 and HSP25 expression in the EDL (A and C) and soleus (B and D) muscles of male HCR/LCR rats after HT. Rats were fed a chow diet or underwent a 3-day HFD challenge and received either a single in vivo ST (37°C) or HT (41°C). Protein levels were normalized to α -tubulin protein levels. White bars represent chow-ST, black bars represent chow-HT, white-hatched bars represent HFD-ST, and gray-hatched bars represent HFD-HT. * $P < 0.01$, ** $P < 0.001$ denotes significant main effect of treatment; † $P < 0.05$ denotes a significant diet \times treatment interaction determined by two-way ANOVA performed in HCR/LCR rats separately; # $P < 0.05$ denotes significantly different between HCR/LCR rats by one-way ANOVA. Values are reported as the mean \pm SE. $N = 5$ –6 samples/group.

not different between HCR/LCR rats (Open bars, Fig. 2A and B). This pattern of greater constitutive HSP72 expression in HCR glycolytic muscles was also observed in the glycolytic white gastrocnemius muscle (data not shown). As was observed in the oxidative soleus muscle, HSP72 expression levels were not different between HCR and LCR rats in the more oxidative red gastrocnemius muscle. 24 h after HT, there was no increase in total HSP25 levels in either the EDL or soleus muscles from HCR and LCR rats (Fig. 2C and D). In addition, constitutive HSP25 levels were not different between HCR/LCR rats in the EDL or soleus.

The Ability of HT to Increase Insulin-Stimulated Glucose Uptake Is Lost in the Absence of HSP72 Activation

In order to demonstrate that the effects of HT on insulin-stimulated glucose uptake occur due to activation of HSP72,

primary myotubes from HCR and LCR rats were transfected with siHSP72 to block further expression/accumulation of HSP72 after HT. In myotubes transfected with control siRNA (siCTL), insulin-stimulated glucose uptake was increased in both HCR and LCR myotubes 24 h after HT (Fig. 3A and B). In siHSP72-treated myotubes (with a resulting decrease in HSP72 induction of 40% and 33% in HCR and LCR, respectively) (Fig. 3C and D), the ability of HT to increase insulin-stimulated glucose uptake was eliminated. HSP25 levels did not change in response to siHSP72, demonstrating the targeted degradation of HSP72 mRNA with this approach (Fig. 3E and F).

HT Decreases Triglyceride Accumulation in LCR Muscle

Increases in intramuscular lipid storage are intimately linked to reduced skeletal muscle insulin sensitivity (31) and therefore we examined intramuscular triglyceride content

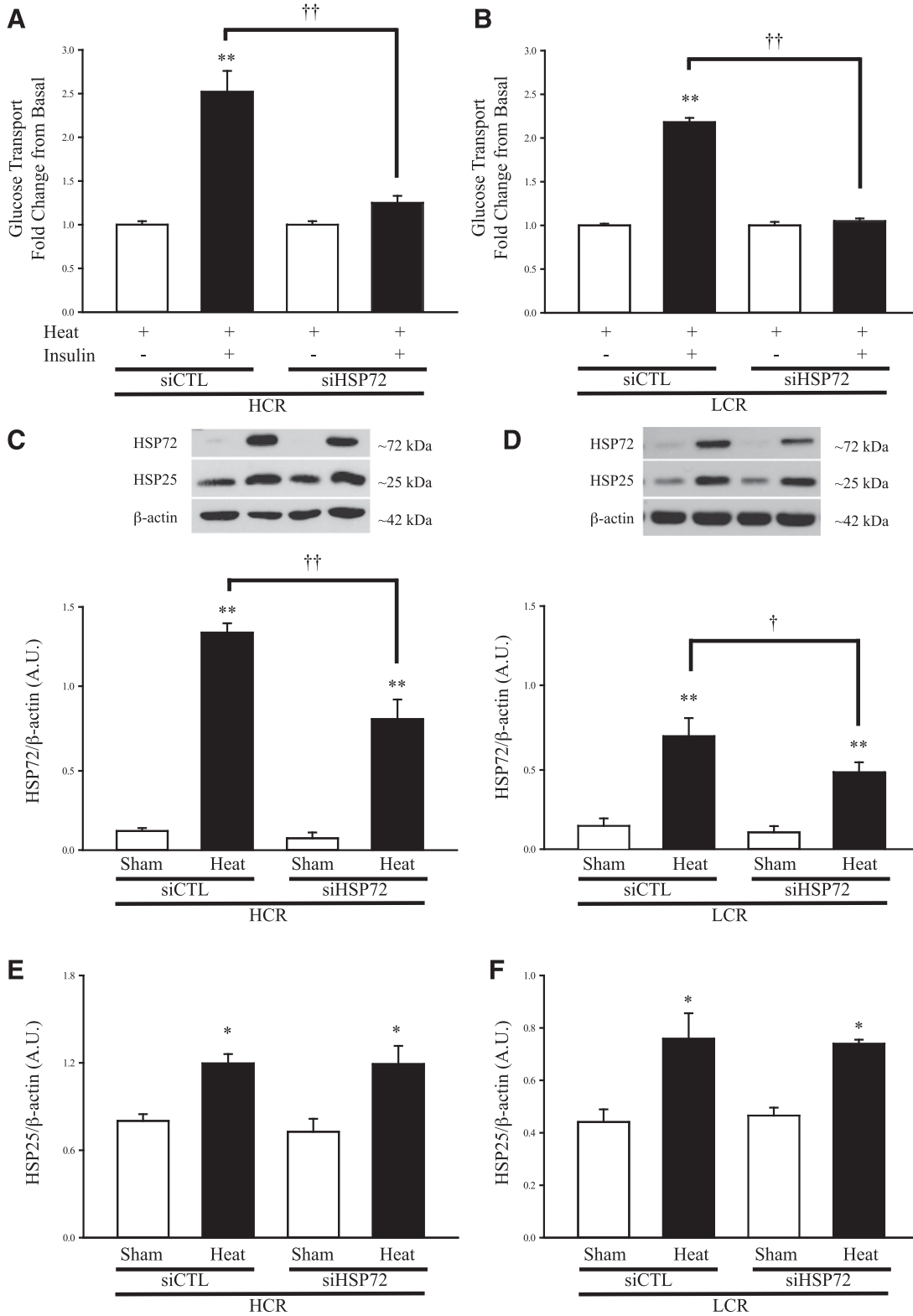


Figure 3—Glucose transport and HSP response in primary myotubes isolated from HCR/LCR rats with decreased induction of HSP72. Insulin-stimulated glucose uptake 24 h after a single in vitro HT (42°C, 30 min) of primary myotubes isolated from adult male HCR (A) and LCR rats (B). Primary myotubes were isolated, transfected with siCTL or siHSP72 to disrupt the induction of HSP72, received a single HT 24 h after transfection; and 24 h after HT underwent insulin-stimulated glucose uptake experiments. Western blots of HSP72 (C and D) and HSP25 (E and F) expression after ST (37°C, 30 min) or HT and transfection with siHSP72 or siCTL in primary myotubes isolated from HCR/LCR rats. Protein levels were normalized to β-actin protein levels. **P* < 0.01, ***P* < 0.001 denotes significantly increased from basal condition or ST; †*P* < 0.05, ††*P* < 0.001 denotes significantly different from siCTL determined by one-way ANOVA. Values are reported as the mean ± SE. *N* = 6 samples/condition.

in the white (glycolytic) and red (oxidative) gastrocnemius. Triglyceride content increased only in the white gastrocnemius after a 3-day HFD in LCR rats (Fig. 4A). There was a trend for an increase in triglyceride content in red gastrocnemius from LCR rats ($P = 0.062$) and HT effectively decreased intramuscular triglyceride content in this oxidative muscle (Fig. 4B).

Diet and HT Effects in the Liver From HCR/LCR Rats

Because previous studies have demonstrated a significant, and perhaps dominant, effect on the liver with a 3-day HFD (32,33), we examined the impact of HT after a 3-day HFD in the liver from HCR/LCR rats. As previously described (22), liver triglyceride content was greater in the LCR rats compared with HCR rats fed a chow diet (Fig. 5A). In LCR rats, HT reduced liver triglyceride content in both chow and HF-fed animals. HT did not alter liver triglyceride content in HCR rats.

Liver HSP72 and HSP25 were increased after HT in both HCR and LCR rats (Fig. 5B and C). Interestingly, induction of hepatic HSP72 was greater in LCR rats compared with HCR rats fed a chow diet. However, induction of both HSP72 and HSP25 in the liver was reduced after a 3-day HFD in LCR rats. HSP induction was unaffected by diet in HCR rats. Constitutive expression of liver HSP72 did not differ between HCR and LCR rats. However, HSP25 protein content was greater in liver from HCR rats compared with LCR rats (open bars, Fig. 5C).

Diet and HT Effects in Adipose Tissue From HCR/LCR Rats

Adipocyte cross-sectional area from eWAT was greater in the LCR rats compared with HCR rats (Fig. 5D and E). While there was no effect of the 3-day HFD on adipocyte size in either strain, HT decreased adipocyte size in LCR rats. HSP72 is induced with HT in eWAT from HCR and

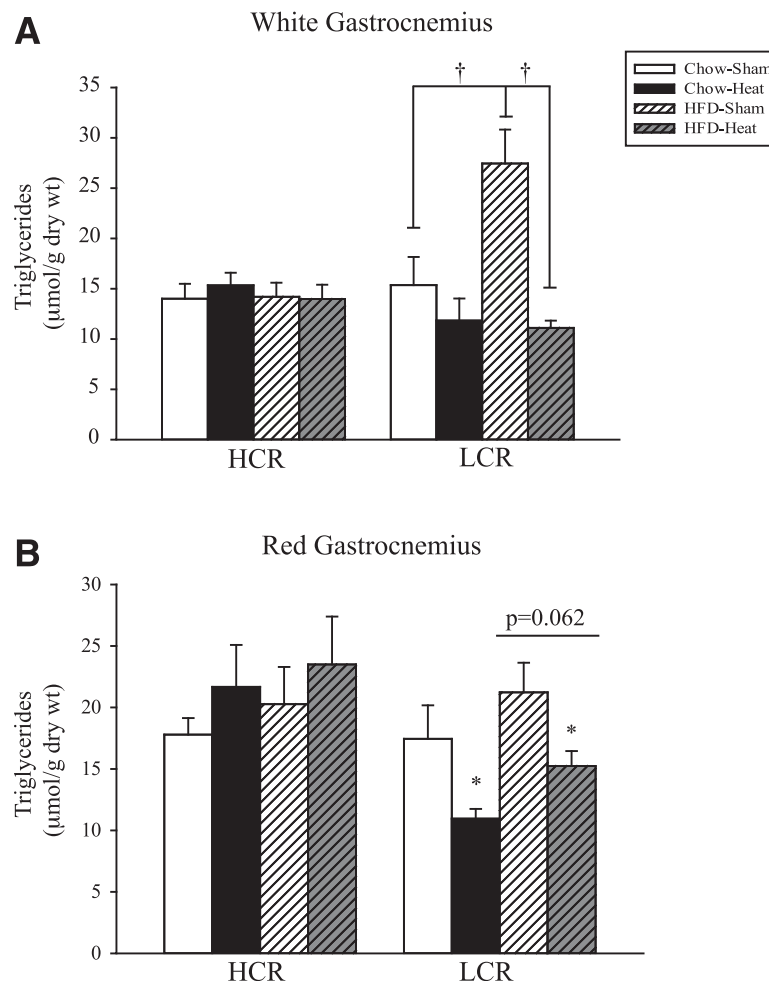


Figure 4—Triglyceride content of white and red gastrocnemius muscles of HCR/LCR rats. Intramuscular triglyceride content of white (A) and red (B) gastrocnemius muscles of male HCR/LCR rats after HT. Rats were fed a chow diet or underwent a 3-day HFD challenge and received either a single in vivo ST (37°C) or HT (41°C). White bars represent chow-ST, black bars represent chow-HT, white-hatched bars represent HFD-ST, and gray-hatched bars represent HFD-HT. * $P < 0.01$ denotes a significant main effect of HT; † $P < 0.05$ denotes a significant diet \times treatment interaction whereby triglyceride content of HFD-ST LCR rats is significantly greater than chow-ST LCR rats and HFD-HT LCR rats determined by two-way ANOVA. There was a trend ($P = 0.062$) toward a main effect of diet in LCR rats. Values are reported as the mean \pm SE. $N = 4$ –6 samples/group.

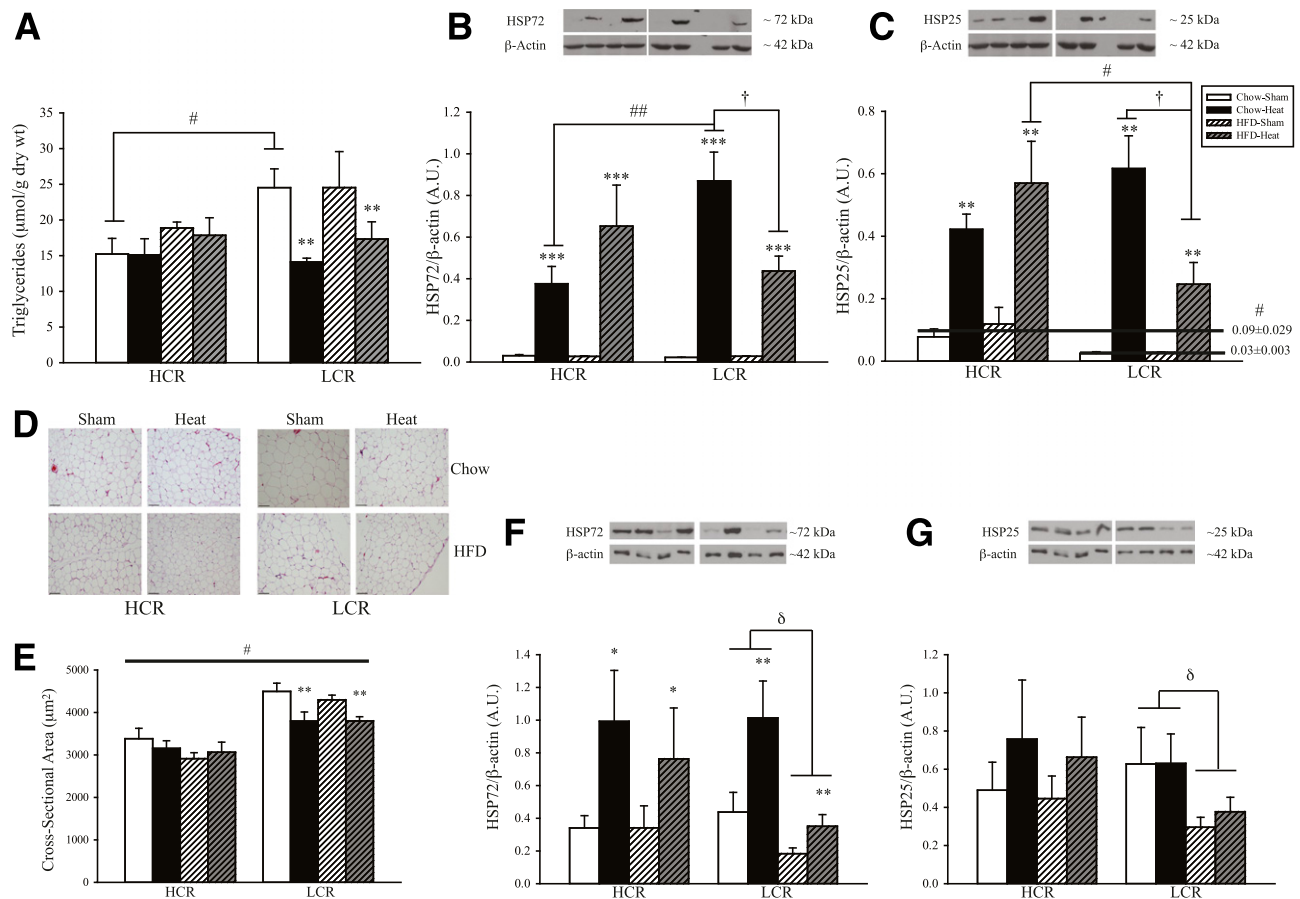


Figure 5—Liver and adipose tissue response to HT in HCR/LCR rats. Triglyceride content (A) and HSP72 (B) and HSP25 expression in liver (C); representative images of cross-sections of eWAT (D); cross-sectional area of adipocytes (E); and HSP72 (F) and HSP25 (G) expression in eWAT of HCR/LCR rats. Rats were fed a chow diet or underwent a 3-day HFD challenge and received either a single *in vivo* ST (37°C) or HT (41°C). Protein levels were normalized to β -actin protein levels. White bars represent chow-ST, black bars represent chow-HT, white-hatched bars represent HFD-ST, and gray-hatched bars represent HFD-HT. * $P < 0.05$, ** $P < 0.01$, *** $P < 0.001$ denote a significant main effect of treatment; $\delta P < 0.01$ denotes a significant main effect of diet; $\dagger P < 0.01$ denotes a significant diet \times treatment interaction determined by two-way ANOVA performed in HCR/LCR rats separately; # $P < 0.05$ and ## $P < 0.01$ denote significantly different from HCR rats of corresponding treatment group by one-way ANOVA. Values are reported as the mean \pm SE. $N = 4$ –6 animals/ group.

LCR rats, however induction and constitutive levels are blunted by a 3-day HFD in the LCR only (Fig. 5F). The HFD decreased expression of HSP25 in eWAT from LCR rats (Fig. 5G). Induction of HSP25 was not impacted by diet or HT in eWAT from HCR rats.

DISCUSSION

New findings from the current study demonstrate the ability of a short-term HT to mitigate metabolic dysfunction in muscle, liver, and adipose tissue after a 3-day HFD. Unlike previous studies demonstrating the benefits of HT and transgenic overexpression of HSP72 against an HFD (13–17), this is the first study to consider the effects of HSP induction in a model with intrinsically low and high aerobic capacity. LCR rats develop skeletal muscle insulin resistance and increase triglyceride stores only in glycolytic muscles after a 3-day HFD, whereas HCR rats are protected from short-term metabolic insult. In the absence of HSP72 induction in HCR and LCR primary myotubes, HT has no effect on insulin-stimulated glucose

uptake, a finding that suggests the beneficial metabolic effects of HT occur through HSP72. Previous studies have demonstrated an early effect of diet on the liver; however, to our knowledge, our findings are the first to demonstrate metabolic defects in skeletal muscle as a result of a 3-day HFD. Adipocyte size and triglyceride storage in the liver were also decreased with a single HT, demonstrating beneficial metabolic adaptations in multiple tissues. The mechanisms by which low aerobic capacity leads to increased susceptibility to metabolic disease, and by which high aerobic capacity plays a protective role, have not been elucidated. Our novel findings suggest that a deficiency in the heat shock response may underlie increased susceptibility to metabolic disease with low aerobic capacity.

Previous studies have demonstrated an important association between HSP72 expression levels and metabolic disease. Constitutive levels of HSP72 and the primary HSP transcription factor HSF-1 are lower in the skeletal muscle of patients with type 2 diabetes and of insulin-resistant rodents (12,13,34–37). As a model of low intrinsic

aerobic capacity, LCR rats display symptomology of metabolic syndrome with reduced whole-body and skeletal muscle insulin sensitivity shown here and elsewhere (18–24). Karvinen et al. (38) assessed HSPs in aging HCR/LCR muscles; however, this is the first study to fully characterize constitutive expression of HSPs in metabolic tissue of HCR and LCR rats. HSP72 was higher in HCR rats compared with LCR rats, but only in glycolytic skeletal muscles. Previously, we have shown that HSP72 protein expression is associated with oxidative capacity and that expression levels are highest in slow-twitch muscles like the soleus, compared with glycolytic muscles like the EDL (39). In addition, HSP expression levels are highest in WAT depots with greater oxidative capacity (9). It may therefore be a positive adaptation of HCR rats to have increased HSP72 expression in glycolytic muscles as protection from metabolic insult. Interestingly, the only other difference in constitutive HSP expression levels between HCR and LCR rats observed was HSP25 in the liver. Very little is known about the mechanisms of HSPs in liver metabolism, thus the potential for HSP25 expression to be protective in the livers of HCR rats requires further investigation.

Induction of HSP72 after HT was blunted in skeletal muscle, liver, and adipose tissue from LCR rats, findings that correspond with the HSP response in insulin-resistant or diabetic animals (36,40). Blunting HSP72 activation in HCR and LCR primary myotubes via siRNA eliminated the ability of HT to increase insulin-stimulated glucose uptake, further highlighting the importance of HSP72 induction in mediating the beneficial effects of HT in skeletal muscle (these findings were repeated and confirmed in another rat strain) (Supplementary Fig. 2). The induction of HSP72 was greater in the liver of chow-fed LCR rats compared with chow-fed HCR rats after HT, perhaps indicating that the stress response is heightened in the liver of the LCR rat. HSP72 and HSP25 induction was blunted in the livers of LCR rats after a 3-day HFD challenge, suggesting that additional metabolic insult weakens this stress response in LCR rats, whereas the HCR stress response is unchanged. Overall, we saw improvements in blood glucose, insulin-stimulated glucose uptake, and triglyceride storage in liver and muscle; and decreased adipocyte size with short-term HT of LCR rats, highlighting the effectiveness of *in vivo* HT on metabolic outcomes. We predict that decreased HSP activation in LCR glycolytic muscle and liver with the 3-day HFD could be indicators of heightened susceptibility to future chronic metabolic stress and/or metabolic disease progression. Interestingly, mice with a condition akin to Huntington disease are able to elicit a heat shock response early in the disease (increased HSP72 and HSP25 expression in the brain), but this becomes impaired with disease progression (41). Additional studies examining the impact of long-term high-fat feeding and oxidative stress/aging on the heat shock response are warranted.

High-fat feeding has been shown to increase the acetylation of lysine residues in skeletal muscle and liver (42), and acetylation of HSF-1 reduces its DNA binding activity and ability to induce HSPs. Sirt1 has been shown to directly deacetylate HSF-1, allowing for longer DNA binding and enhanced HSP production (43). In the current study, we observed lower Sirt1 levels in the white gastrocnemius muscles of LCR rats, corresponding with decreased HSF-1, HSP72, and the mitochondrial HSP, HSP60, in these muscles (Supplementary Fig. 1). In addition to acetylation, HSF-1 can be inhibited through phosphorylation by stress kinases, such as glycogen synthase kinase 3, extracellular signal-related kinase, and c-Jun N-terminal kinase (44,45), proteins that tend to be increased with long-term HFD consumption (46,47). The response of HSP72 and HSP25 to heat and diet were dissimilar in muscle and adipose tissue, with only the liver showing a consistent pattern of change in both proteins. Few studies have extensively examined HSP72 and HSP25; however, the Locke laboratory also demonstrated a differential response of the two HSPs in a model of streptozotocin-induced diabetes (48). HSP72 and HSP25 are products of different genes (*Hspa1a/b* and *Hspb1* encoding HSP72 and HSP25, respectively), and differential binding of HSF-1 to target heat shock gene promoters may occur in response to HFD consumption. Reduced HSF-1 promoter binding to *Hspa1a/b* or *Hspb1* could be influenced by the DNA binding competency of HSF-1 itself or by the chromatin architecture and accessibility of specific heat shock promoters (41). Future studies examining the nucleosome landscape of HSF-1 promoter binding would help address these questions.

Previously, Morris et al. (22) reported that LCR rats display metabolic inflexibility when fed an HFD for 3 days, results that were associated with the development of hepatic steatosis. Our data expand upon this concept by showing that, when fed an HFD for 3 days, LCR rats have decreased insulin sensitivity in glycolytic muscle and additional fatty acids are stored as excess triglycerides. In contrast, HCR rats have been shown to selectively partition fatty acids into skeletal muscle while also demonstrating increased whole body fatty acid oxidation (22). Increased triglyceride content in muscle and liver after consumption of an HFD for 3 days in LCR rats may be a result of defective mitochondrial lipid handling. LCR rats have been shown to have lower mitochondrial content and functionality in skeletal muscle and liver compared with HCR rats (18,21,23,24), and in the current study we observed that differences between HCR and LCR rats in the content of the respiratory chain complexes were most pronounced in glycolytic muscles (Supplementary Fig. 1). This is supported by findings from the study by Rivas et al. (24) showing that differences in mitochondrial enzyme activity are more pronounced in LCR/HCR rats in glycolytic muscle compared with oxidative muscle. The improvements in insulin sensitivity (muscle) and triglyceride content (muscle and liver) in LCR rats after HT may represent improvements in mitochondrial function.

The mechanisms by which HSPs protect against insulin resistance are not completely understood, but are likely to be multifactorial. Recently, HSP72 has been shown to be a powerful regulator of mitochondrial function and the processes of autophagy/mitophagy. Overexpression of HSP72 in skeletal muscle results in a nearly 50% increase in mitochondrial content and an approximately twofold increase in endurance running capacity (15), whereas mice lacking HSP72 display whole-body and skeletal muscle insulin resistance, as well as deficits in fatty acid oxidation. Recently, Drew et al. (49) established that HSP72 is essential for proper function of mitophagy, the autophagic process by which damaged mitochondria are cleared (50). Loss of HSP72 results in an increase in levels of Parkin, an E3 ubiquitin ligase thought to be essential for mitophagy (50); however, the available Parkin is thought to be unable to translocate to the mitochondria properly and to target dysfunctional mitochondria for degradation through mitophagy (49). Our data further support this idea, because glycolytic muscles from LCR rats with reduced HSP72 levels also had increased Parkin levels (Supplementary Fig. 1). Future investigations are needed to determine the potential of HSP72 to mediate mitophagy processes.

In conclusion, our new findings demonstrate that HT can mitigate HFD-induced metabolic dysfunction in rats with low aerobic capacity. The known functions of HSP72 to improve insulin action and to enhance mitochondrial function and quality could underlie this protective effect of HT, and additional studies are needed to elucidate these mechanisms. However, our findings clearly illustrate that skeletal muscle, liver, and adipose tissue from LCR rats all display a blunted HSP induction as the result of consuming an HFD for 3 days. This could indicate an early and heightened susceptibility to metabolic insult in this model as a result of a decreased stress response. Targeted induction of HSPs could be a preventive approach for maintaining the natural stress response of the body and preventing metabolic disease.

Acknowledgments. The authors thank Molly Kalahar and Lori Heckenkamp from the University of Michigan for their expert care of the rat colony. The authors also thank Dr. Norberto C. Gonzalez from the University of Kansas Medical Center for his intellectual contributions to this research and understanding of the high-capacity runner/low-capacity runner model. In addition, the authors thank Camron Myers and Michael Cooper from the University of Kansas Medical Center for their assistance with this project.

Funding. This work was supported by National Institutes of Health (NIH)/National Institute on Aging grant AG-031575 (to P.C.G.); NIH/National Institute of Diabetes and Digestive and Kidney Diseases grant DK-088940 (to J.P.T.) and DK-077200; NIH grant 5-T32-AR-48523-8 (to E.M.M.); a University of Kansas Medical Center Biomedical Research Training Program Predoctoral Fellowship (to R.S.R.); National Institute of General Medical Sciences grant GM-104194; and National Center for Research Resources grant ROD012098A. Core support was provided by Eunice Kennedy Shriver National Institute of Child Health and Human Development grant HD-002528. The low-capacity runner/high-capacity runner rat model system was funded by Office of Research Infrastructure Programs grant P40-OD-021331 (to L.G.K. and S.L.B.) from the NIH. These rat models are maintained as an international resource with support from the Department of

Anesthesiology at the University of Michigan, Ann Arbor, MI (<http://koch-britton.med.umich.edu/>). This work was supported with resources and the use of facilities at the Harry S. Truman Memorial VA Hospital in Columbia, MO.

Duality of Interest. No potential conflicts of interest relevant to this article were reported.

Author Contributions. R.S.R. designed and conducted the experiments, analyzed the data, and wrote and edited the manuscript. E.M.M. designed and conducted the experiments. J.L.W., A.E.A., C.S.M., K.S.W., D.R.W., and G.M.E.M. conducted the experiments. L.G.K. and S.L.B. designed and maintained the high-capacity runner/low-capacity runner animal model. J.P.T. designed the experiments, analyzed the data, and edited the manuscript. P.C.G. designed the experiments, analyzed the data, and wrote and edited the manuscript. P.C.G. is the guarantor of this work and, as such, had full access to all the data in the study and takes responsibility for the integrity of the data and the accuracy of the data analysis.

References

1. Myers J, Prakash M, Froelicher V, Do D, Partington S, Atwood JE. Exercise capacity and mortality among men referred for exercise testing. *N Engl J Med* 2002;346:793–801
2. Kodama S, Saito K, Tanaka S, et al. Cardiorespiratory fitness as a quantitative predictor of all-cause mortality and cardiovascular events in healthy men and women: a meta-analysis. *JAMA* 2009;301:2024–2035
3. Kokkinos P, Myers J, Faselis C, et al. Exercise capacity and mortality in older men: a 20-year follow-up study. *Circulation* 2010;122:790–797
4. Church TS, Cheng YJ, Earnest CP, et al. Exercise capacity and body composition as predictors of mortality among men with diabetes. *Diabetes Care* 2004;27:83–88
5. LaMonte MJ, Barlow CE, Jurca R, Kampert JB, Church TS, Blair SN. Cardiorespiratory fitness is inversely associated with the incidence of metabolic syndrome: a prospective study of men and women. *Circulation* 2005;112:505–512
6. Bouchard C, Dionne FT, Simoneau JA, Boulay MR. Genetics of aerobic and anaerobic performances. *Exerc Sport Sci Rev* 1992;20:27–58
7. Bombardier E, Vigna C, Iqbal S, Tiidus PM, Tupling AR. Effects of ovarian sex hormones and downhill running on fiber-type-specific HSP70 expression in rat soleus. *J Appl Physiol* (1985) 2009;106:2009–2015
8. Locke M, Noble EG, Atkinson BG. Inducible isoform of HSP70 is constitutively expressed in a muscle fiber type specific pattern. *Am J Physiol* 1991;261:C774–C779
9. Rogers RS, Beaudoin MS, Wheatley JL, Wright DC, Geiger PC. Heat shock proteins: in vivo heat treatments reveal adipose tissue depot-specific effects. *J Appl Physiol* 2015;118:98–106
10. Akerfelt M, Morimoto RI, Sistonen L. Heat shock factors: integrators of cell stress, development and lifespan. *Nat Rev Mol Cell Biol* 2010;11:545–555
11. Morimoto RI. Regulation of the heat shock transcriptional response: cross talk between a family of heat shock factors, molecular chaperones, and negative regulators. *Genes Dev* 1998;12:3788–3796
12. Kurucz I, Morva A, Vaag A, et al. Decreased expression of heat shock protein 72 in skeletal muscle of patients with type 2 diabetes correlates with insulin resistance. *Diabetes* 2002;51:1102–1109
13. Chung J, Nguyen AK, Henstridge DC, et al. HSP72 protects against obesity-induced insulin resistance. *Proc Natl Acad Sci USA* 2008;105:1739–1744
14. Gupte AA, Bomhoff GL, Swerdlow RH, Geiger PC. Heat treatment improves glucose tolerance and prevents skeletal muscle insulin resistance in rats fed a high-fat diet. *Diabetes* 2009;58:567–578
15. Henstridge DC, Bruce CR, Drew BG, et al. Activating HSP72 in rodent skeletal muscle increases mitochondrial number and oxidative capacity and decreases insulin resistance. *Diabetes* 2014;63:1881–1894
16. Literáti-Nagy B, Kulcsár E, Literáti-Nagy Z, et al. Improvement of insulin sensitivity by a novel drug, BGP-15, in insulin-resistant patients: a proof of

- concept randomized double-blind clinical trial. *Horm Metab Res* 2009;41:374–380
17. Adachi H, Kondo T, Ogawa R, et al. An acyclic polyisoprenoid derivative, geranylgeranylacetone protects against visceral adiposity and insulin resistance in high-fat-fed mice. *Am J Physiol Endocrinol Metab* 2010;299:E764–E771
18. Noland RC, Thyfault JP, Henes ST, et al. Artificial selection for high-capacity endurance running is protective against high-fat diet-induced insulin resistance. *Am J Physiol Endocrinol Metab* 2007;293:E31–E41
19. Novak CM, Escande C, Burghardt PR, et al. Spontaneous activity, economy of activity, and resistance to diet-induced obesity in rats bred for high intrinsic aerobic capacity. *Horm Behav* 2010;58:355–367
20. Thyfault JP, Rector RS, Uptergrove GM, et al. Rats selectively bred for low aerobic capacity have reduced hepatic mitochondrial oxidative capacity and susceptibility to hepatic steatosis and injury. *J Physiol* 2009;587:1805–1816
21. Lessard SJ, Rivas DA, Stephenson EJ, et al. Exercise training reverses impaired skeletal muscle metabolism induced by artificial selection for low aerobic capacity. *Am J Physiol Regul Integr Comp Physiol* 2011;300:R175–R182
22. Morris EM, Jackman MR, Johnson GC, et al. Intrinsic aerobic capacity impacts susceptibility to acute high-fat diet-induced hepatic steatosis. *Am J Physiol Endocrinol Metab* 2014;307:E355–E364
23. Wisløff U, Najjar SM, Ellingsen O, et al. Cardiovascular risk factors emerge after artificial selection for low aerobic capacity. *Science* 2005;307:418–420
24. Rivas DA, Lessard SJ, Saito M, et al. Low intrinsic running capacity is associated with reduced skeletal muscle substrate oxidation and lower mitochondrial content in white skeletal muscle. *Am J Physiol Regul Integr Comp Physiol* 2011;300:R835–R843
25. Koch LG, Britton SL. Artificial selection for intrinsic aerobic endurance running capacity in rats. *Physiol Genomics* 2001;5:45–52
26. Zuurbier CJ, Keijzers PJ, Koeman A, Van Wezel HB, Hollmann MW. Anesthesia's effects on plasma glucose and insulin and cardiac hexokinase at similar hemodynamics and without major surgical stress in fed rats. *Anesth Analg* 2008;106:135–142
27. Frayn KN, Maycock PF. Skeletal muscle triacylglycerol in the rat: methods for sampling and measurement, and studies of biological variability. *J Lipid Res* 1980;21:139–144
28. Rector RS, Thyfault JP, Morris RT, et al. Daily exercise increases hepatic fatty acid oxidation and prevents steatosis in Otsuka Long-Evans Tokushima Fatty rats. *Am J Physiol Gastrointest Liver Physiol* 2008;294:G619–G626
29. Hirabara SM, Silveira LR, Alberici LC, et al. Acute effect of fatty acids on metabolism and mitochondrial coupling in skeletal muscle. *Biochim Biophys Acta* 2006;1757:57–66
30. Gupte AA, Bomhoff GL, Touchberry CD, Geiger PC. Acute heat treatment improves insulin-stimulated glucose uptake in aged skeletal muscle. *J Appl Physiol* (1985) 2011;110:451–457
31. Muoio DM. Revisiting the connection between intramyocellular lipids and insulin resistance: a long and winding road. *Diabetologia* 2012;55:2551–2554
32. Kraegen EW, Clark PW, Jenkins AB, Daley EA, Chisholm DJ, Storlien LH. Development of muscle insulin resistance after liver insulin resistance in high-fat-fed rats. *Diabetes* 1991;40:1397–1403
33. Samuel VT, Liu ZX, Qu X, et al. Mechanism of hepatic insulin resistance in non-alcoholic fatty liver disease. *J Biol Chem* 2004;279:32345–32353
34. Bruce CR, Carey AL, Hawley JA, Febbraio MA. Intramuscular heat shock protein 72 and heme oxygenase-1 mRNA are reduced in patients with type 2 diabetes: evidence that insulin resistance is associated with a disturbed antioxidant defense mechanism. *Diabetes* 2003;52:2338–2345
35. Rodrigues-Krause J, Krause M, O'Hagan C, et al. Divergence of intracellular and extracellular HSP72 in type 2 diabetes: does fat matter? *Cell Stress Chaperones* 2012;17:293–302
36. Atalay M, Oksala NK, Laaksonen DE, et al. Exercise training modulates heat shock protein response in diabetic rats. *J Appl Physiol* (1985) 2004;97:605–611
37. Patti ME, Butte AJ, Crunkhorn S, et al. Coordinated reduction of genes of oxidative metabolism in humans with insulin resistance and diabetes: potential role of PGC1 and NRF1. *Proc Natl Acad Sci USA* 2003;100:8466–8471
38. Karvinen S, Silvennoinen M, Vainio P, et al. Effects of intrinsic aerobic capacity, aging and voluntary running on skeletal muscle sirtuins and heat shock proteins. *Exp Gerontol* 2016;79:46–54
39. Gupte AA, Bomhoff GL, Geiger PC. Age-related differences in skeletal muscle insulin signaling: the role of stress kinases and heat shock proteins. *J Appl Physiol* (1985) 2008;105:839–848
40. Kavanagh K, Wylie AT, Chavanne TJ, et al. Aging does not reduce heat shock protein 70 in the absence of chronic insulin resistance. *J Gerontol A Biol Sci Med Sci* 2012;67:1014–1021
41. Labbadia J, Cunliffe H, Weiss A, et al. Altered chromatin architecture underlies progressive impairment of the heat shock response in mouse models of Huntington disease. *J Clin Invest* 2011;121:3306–3319
42. Muoio DM. Metabolic inflexibility: when mitochondrial indecision leads to metabolic gridlock. *Cell* 2014;159:1253–1262
43. Westerheide SD, Anckar J, Stevens SM Jr, Sistonen L, Morimoto RI. Stress-inducible regulation of heat shock factor 1 by the deacetylase SIRT1. *Science* 2009;323:1063–1066
44. Chu B, Soncin F, Price BD, Stevenson MA, Calderwood SK. Sequential phosphorylation by mitogen-activated protein kinase and glycogen synthase kinase 3 represses transcriptional activation by heat shock factor-1. *J Biol Chem* 1996;271:30847–30857
45. Park J, Liu AY. JNK phosphorylates the HSF1 transcriptional activation domain: role of JNK in the regulation of the heat shock response. *J Cell Biochem* 2001;82:326–338
46. Vinayagamoorthi R, Bobby Z, Sridhar MG. Antioxidants preserve redox balance and inhibit c-Jun-N-terminal kinase pathway while improving insulin signaling in fat-fed rats: evidence for the role of oxidative stress on IRS-1 serine phosphorylation and insulin resistance. *J Endocrinol* 2008;197:287–296
47. Wellen KE, Hotamisligil GS. Inflammation, stress, and diabetes. *J Clin Invest* 2005;115:1111–1119
48. Najemnikova E, Rodgers CD, Locke M. Altered heat stress response following streptozotocin-induced diabetes. *Cell Stress Chaperones* 2007;12:342–352
49. Drew BG, Ribas V, Le JA, et al. HSP72 is a mitochondrial stress sensor critical for Parkin action, oxidative metabolism, and insulin sensitivity in skeletal muscle. *Diabetes* 2014;63:1488–1505
50. Ding WX, Yin XM. Mitophagy: mechanisms, pathophysiological roles, and analysis. *Biol Chem* 2012;393:547–564